Synaptic plasticity in a cerebellum-like structure depends on temporal order

Curtis C. Bell*, Victor Z. Han*, Yoshiko Sugawara† & Kirsty Grant‡

* *R. S. Dow Neurological Sciences Institute, Good Samaritan Hospital and Medical Center, 1120 N.W. 20th Avenue, Portland, Oregon 97209, USA*
† *Institut Alfred Fessard, CNRS 91190 Gif-sur-Yvette, France*
‡ *Department of Physiology, Teikyo University School of Medicine, Kaga 2-11-1, Itabashi-ku, Tokyo 173, Japan*

Cerebellum-like structures in fish appear to act as adaptive sensory processors, in which learned predictions about sensory input are generated and subtracted from actual sensory input, allowing unpredicted inputs to stand out[1–3]. Pairing sensory input with centrally originating predictive signals, such as corollary discharge signals linked to motor commands, results in neural responses to the predictive signals alone that are 'negative images' of the previously paired sensory responses. Adding these 'negative images' to actual sensory inputs minimizes the neural response to predictable sensory features. At the cellular level, sensory input is relayed to the basal region of Purkinje-like cells, whereas predictive signals are relayed by parallel fibres to the apical dendrites of the same cells[4]. The generation of negative images could be explained by plasticity at parallel fibre synapses[5–7]. We show here that such plasticity exists in the electrosensory lobe of mormyrid electric fish and that it has the necessary properties for such a model: it is reversible, anti-hebbian (excitatory postsynaptic potentials (EPSPs) are depressed after pairing with a postsynaptic spike) and tightly dependent on the sequence of pre- and postsynaptic events, with depression occurring only if the postsynaptic spike follows EPSP onset within 60 ms.

Plasticity at parallel fibre synapses was tested in an *in vitro* slice preparation from the electrosensory lobe of the mormyrid electric fish *Gnathonemus petersii*. Afferents from electroreceptors terminate in the electrosensory lobe (Fig. 1a). All recordings were taken from GABAergic Purkinje-like cells[8,9] (Fig. 1a, inset) which are also known as medium ganglion cells (47 cells; mean membrane potential, 62 mV; range, 53–80 mV; s.e.m., 1.2 mV). Recordings from these cells show large broad spikes (40–60 mV, 8–15 ms; Fig. 1b) that probably arise in the apical dendrites. The spikes are sodium rather than calcium spikes because they are blocked by tetrodotoxin but are still present in a medium with zero calcium and/or cadmium (200 μM) to block calcium channels (7 cells; Fig. 1b). A previous *in vivo* study indicated that the occurrence of the broad spikes is necessary for a plastic change in the response of these cells to a corollary discharge linked to the motor command that elicits the electric organ discharge[5].

Transverse slices of ELL were prepared and two stimulating electrodes (S1 and S2) were placed in the molecular layer to activate separate sets of parallel fibres (Fig. 1a). Parallel fibre stimuli evoke an EPSP lasting for 30 to 60 ms (Fig. 1b) or an EPSP followed by an inhibitory postsynaptic potential (IPSP; mean EPSP amplitude before any pairings, 2.8 mV; range, 0.2–6.8 mV; s.e.m., 0.24 mV). S1 and S2 parallel fibre inputs were stimulated with a fixed interval of 500 or 250 ms between them at a rate of 0.1 Hz during control periods before and after pairing, and at a rate of either 1 Hz (42 cells with an S1–S2 interval of 500 ms) or 2 Hz (5 cells with an S1–S2 interval of 250 ms) during pairing. During a pairing, the broad spike was evoked at a fixed moment in the cycle by a 20-ms depolarizing current pulse to the postsynaptic cell. No differences were observed between pairings at 1 and 2 Hz and the data from these two protocols was pooled. Pairing was maintained for 6 min (360 pairings at 1 Hz) and as many as six different pairings were carried out in the same cell, each pairing with a different timing relation between the intracellularly evoked broad spike and stimulation of the S1 and S2 parallel fibre inputs. Two types of controls were carried out: a 'broad spikes only' control in which the postsynaptic broad spikes were evoked at 1 Hz with no concomitant parallel fibres EPSPs; and an 'EPSPS only' control, in which the parallel fibre EPSPs were evoked by S1 and S2 at 1 Hz, with no concomitant postsynaptic broad spike. Parallel fibre EPSP amplitudes were measured for 6–15 min before and after pairings and controls. Differences were tested for significance using the two tailed Student's *t*-test.

Most pairings resulted in significant changes in EPSP amplitude. Forty three of the 47 cells tested had at least one pairing with a significant change in EPSP size. Figure 2A shows a pairing in which the broad spike was evoked 30 ms after the onset of the S1 EPSP and 215 ms before the S2 EPSP. The S1 EPSP decreased after the pairing, whereas the S2 EPSP increased (Fig. 2B).

EPSPs evoked by the same parallel fibre stimulus could increase or decrease in amplitude, depending on the timing relation to the

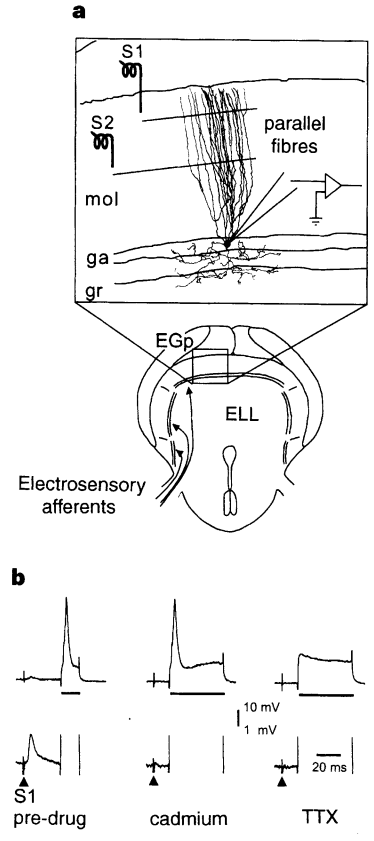

Figure 1 Experimental arrangement and demonstration that the broad spike is a sodium spike. **a**, Transverse section through the electrosensory lobe; inset shows the experimental arrangement. The cell is a reconstruction of a biocytin-filled Purkinje-like neuron. Abbreviations: EGp, eminentia granularis posterior; ELL, electrosensory lobe; ga, gr and mol, ganglionic, granule and molecular layers of the electrosensory lobe, respectively. **b**, Intracellular recording from a Purkinje-like cell showing EPSP evoked by S1 stimulus (arrowhead) and broad spike evoked by intracellular current pulses (bars below upper traces indicate 0.4, 0.4 and 0.8 nA for left, middle and right columns, respectively). Upper traces are low gain, lower traces are high gain. Bath application of 200 μM cadmium causes the S1-evoked EPSP to disappear within a few minutes but the broad spike is unaffected after 20 min (middle column). The broad spike is blocked within a few minutes by bath application of tetrodotoxin (TTX, 0.5 μM; right column).

broad spike during pairing. The cell shown in Fig. 3, for example, underwent six different pairings (P1–P6; Fig. 3A). The S1 EPSP decreased following pairings in which the broad spike occurred just after the EPSP onset (P2 and P6), but increased after pairings at all other delays (Fig. 3B). Input specificity was shown by the concurrent pairings with S2. The S2 EPSP decreased only after the one pairing (P3) in which the broad spike occurred just after the EPSP onset, but increased or didn't change after pairings at other delays.

Thus, pairings in which the broad spike was delivered between 0 and 60 ms after EPSP onset resulted in EPSP decreases, whereas pairings at other tested delays usually resulted in EPSP increases. Figure 4a summarizes the data for all 188 pairings in the 43 cells which showed at least one significant effect of pairing. The effect of timing is particularly striking for pairings near zero delay (Fig. 4b). Pairings with the broad spike between 0 and 60 ms after EPSP onset yielded depression, whereas pairings with the broad spike between 8 and 90 ms before EPSP onset yielded enhancement. A change in timing of less than 10 ms could change the effect of pairing from depression to enhancement. Neither depression nor enhancement depended on a prior pairing-induced change in the opposite direction.

EPSPs were often followed by IPSPs and changes in IPSP latency or amplitude could affect the measurement of EPSP size, raising the question as to whether plasticity occurs in EPSPs, IPSPs or both. Figure 3C shows three superimposed responses to S1 recorded before pairing 1 (trace a), after pairing 1 (trace b) and after pairing 2 (trace c). Initial positive slopes of the responses were altered by pairing, indicating that the earliest components are changed (Fig. 3C). These early changes probably reflect changes in EPSPs, because the anatomy suggests that only the EPSP is monosynaptic. Plasticity of the EPSP alone was confirmed by recording from 8 cells in which the $GABA_A$ blocker bicuculline (30 μM) was added to the ACSF. Only EPSPs were present and no hyperpolarizations were visible under these conditions. All sixteen pairings with the broad spike occurring 10 to 30 ms after EPSP onset resulted in significant ($P = 0.01$) decreases in EPSP amplitude of 10 to 66% (mean, 36%; s.e.m., 5%), whereas of fifteen pairings with the broad spike occurring 15 to 30 ms before EPSP onset, fourteen resulted in significant increases in EPSP amplitude of 12 to 100% (mean 44%; s.e.m., 6%).

The IPSPs evoked by parallel fibre stimulation in normal artificial cerebrospinal fluid also appeared to change following pairing,

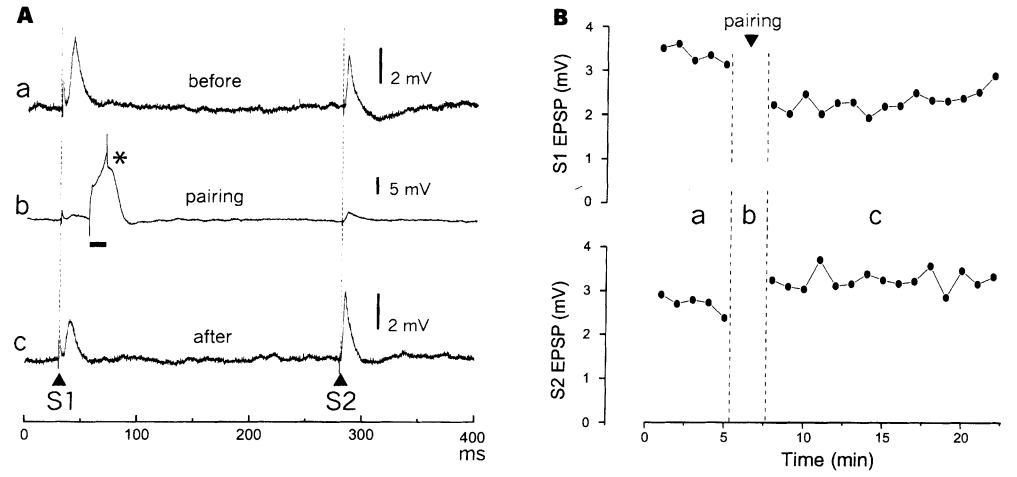

Figure 2 Plasticity of parallel fibre-evoked EPSPs following pairing with a broad spike. **A**, a, Control responses before pairing (average of 6 sweeps). b Pairing of EPSPs with broad spike evoked by intracellular current (indicated by a bar); the broad spike (asterisk) is partially obscured by the artefact of the current pulse (note lower gain.). c, Responses after 6 min of pairing (average of 6 sweeps). **B**, Graphs showing amplitudes (1-min averages) of S1 and S2 responses before (a) and after (c) pairing (b).

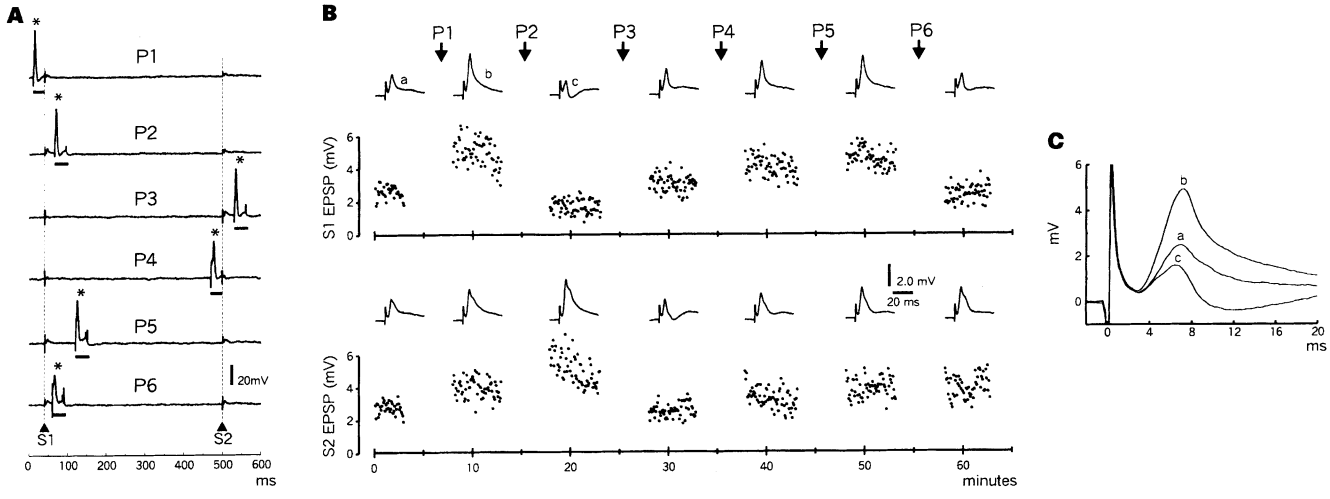

Figure 3 Effects of different pairings in the same cell with different timings of broad spike and EPSPs. **A**, Timing of EPSPs (vertical dashed lines) and broad spike (asterisk). Relative timings of broad spikes with respect to EPSP onset for pairings 1–6 (P1–P6) are as follows (delays with the broad spike after the EPSP are positive and delays with the broad spike before the EPSP are negative): P1 (S1, –29 ms; S2, 490 ms); P2 (S1, 25 ms; S2, –437 ms); P3 (S1, –489 ms; S2, 28 ms); P4 (S1, 429 ms; S2, –32 ms); P5 (S1, 81 ms; S2, 380 ms); P6 (S1, 23 ms; S2, –438 ms). **B**, Graphs showing the peak amplitudes of S1 EPSP (top) and S2 EPSP (bottom) before and after pairings 1–6. Traces above the graphs show the average responses for each period. Traces a, b, and c show responses to S1 before pairing 1, after pairing 1 and after pairing 2, respectively. **C**, Enlarged versions of traces a, b and c are shown superimposed.

increasing when the EPSP decreased and vice versa. Note the appearance of an IPSP to S1 after the second pairing of the cell shown in Fig. 3 (trace c in Fig. 3C) and an IPSP to S2 following pairing 3 (Fig. 3B). Such changes were also seen in cells in which the parallel fibre stimulus evoked a minimal EPSP and a large IPSP. The possibility that an unchanging IPSP is simply unmasked by reduction of the EPSP must still be excluded, however, before plasticity at inhibitory synapses is established.

The EPSP depression observed after pairings in which the broad spike occurred 0 to 60 ms after EPSP onset is clearly an associative effect with a high degree of temporal specificity. The same EPSP was enhanced after pairing at other delays, and a similar EPSP delivered during the same pairing, but at a delay outside this time window, was also enhanced. The degree to which EPSP enhancement by pairing outside this time window is also associative is less clear. Two controls were carried out to control for non-associative factors. When the EPSP was evoked alone at 1 Hz for 6 min there was clear enhancement, but presentation of the broad spike alone at 1 Hz for 6 min had no effect. The enhancement due to giving the EPSP alone was not significantly different from the enhancement after pairings in which the broad spike was delivered at long delays ('Long-delay pairings' in Fig. 4c), or the enhancement after pairings in which the broad spike was delivered just before the EPSP ('short-delay pairings (−50 to 0 ms)' in Fig. 4c). (All eight of the other pairwise comparisons among the five control and experimental groups of Fig. 4c showed significant differences at the 0.01 level, after making the Bonferroni adjustment for multiple comparisons.)

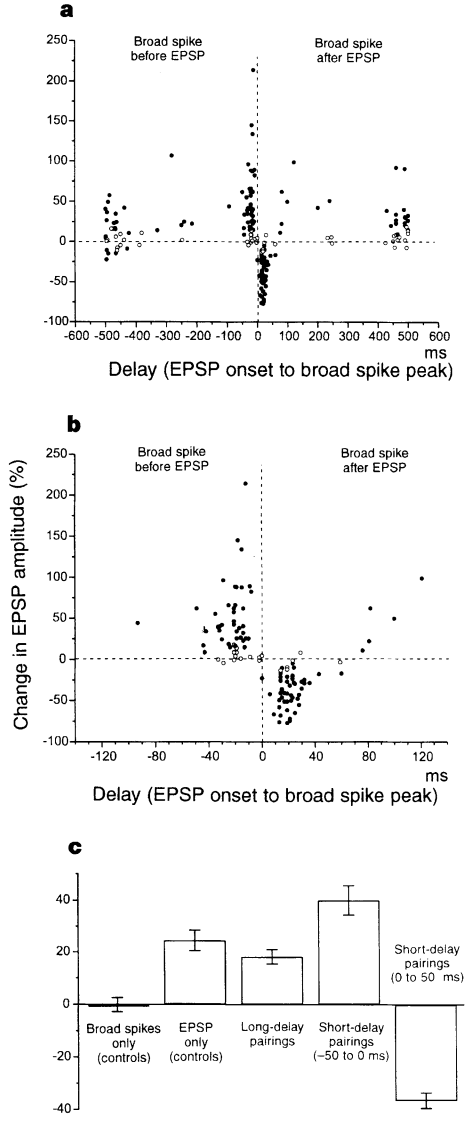

Figure 4 Summary **a**, Percent change in EPSP amplitude plotted against delay between EPSP onset and broad spike peak during pairing. A negative delay with regard to the previous spike and a positive delay with regard to the following spike were present for each pairing. The shorter of these two delays is plotted. Filled circles, significant changes; open circles, non-significant changes (0.01 level). **b**, Same as **a**, but on an expanded scale. **c**, Mean changes in EPSP amplitude following unpaired controls and pairings at different delays (bars show standard error). 'long-delay pairings' includes both positive and negative delays between 300 and 500 ms. The number of controls or pairings was 34, 48, 72, 56 and 51 for the 'broad spike only' control, 'EPSP only' control, long delay pairings, short-delay pairings (−50 to 0 ms), and short-delay pairings (0 to 50 ms, respectively.

The 'EPSP only' control suggests that the enhancements seen with pairings outside the 0–60 ms window might be due to a non-associative effect. A similar non-associative increase in EPSP size following repeated stimulation of parallel fibres alone has been observed in the cerebellum[10,11]. An associative factor might also contribute to the enhancement observed in the mormyrid electrosensory lobe, however. Such a possibility is suggested by *in vivo* results (C.C.B, A. Caputi and K.G., unpublished observations) and the fact that short-delay pairings (−50 to 0 ms) resulted in significantly larger enhancements than long-delay pairings ($P = 0.01$, as described above). Further experiments will be necessary to distinguish an associative effect.

The sharp temporal constraints on pairings that could lead to depression constitute an important result of this study. Work in the hippocampus[12–16] and cerebellum[17–19] has also shown that the magnitude or direction of plastic change at a synapse depends on the temporal relation of pre- and postsynaptic events during pairing. In most of these cases, however, the timing measurements of pre- and postsynaptic events has not been as precise, and temporal constraints have not been as sharp, as in our study. The lack of precise temporal constraints is particularly striking for cerebellar long-term depression, where effective timing relations between presynaptic parallel fibre input and postsynaptic Purkinje cell activation by current injection or climbing fibre input have ranged from presynaptic first by 250 ms (ref. 18) to postsynaptic first by 125 ms (ref. 19). However, dependence on temporal order as tight as in our system has been observed recently in cerebral cortical slices[20]. In the cerebral cortex, in contrast to our results, pairings with the postsynaptic spike given just after EPSP onset resulted in enhancement, whereas pairings with the postsynaptic just before EPSP onset resulted in depression. The fact that the dependence on temporal order was opposite to that observed in our study probably reflects a different type of plasticity in the cerebral cortex from that in the cerebellum or cerebellum-like structures[17].

Our results and the results from cortical slices both indicate that a simple correlation or covariance rule will not always be a sufficient criterion for the occurrence of hebbian or anti-hebbian plasticity. Precise timing and temporal order of individual pre- and postsynaptic events can be critical. Hebb's original statement of his postulate[21] implies the importance of temporal order, but this has often been overlooked in more recent work. A modified rule would state that excitatory inputs that arrive just before a postsynaptic spike (and which could therefore have contributed to the occurrence of the spike during normal operation) are enhanced with hebbian plasticity but depressed with anti-hebbian plasticity. The temporal window of ~60 ms within which pairings with the broad spike lead to depression in our study is similar to the duration of parallel fibre-evoked EPSPs. The results are thus consistent with the idea that inputs that could cause or affect the occurrence of a postsynaptic spike may be treated quite differently from inputs that arrive too early or too late to have such an effect.

The plasticity shown here *in vitro* shares many properties with the plasticity observed *in vivo* following the pairing of a predictive signal with sensory input or intracellular current pulses[1–6]. In both cases, the changes are input-specific, bidirectional and established within a few minutes. In both cases the plasticity is anti-hebbian, with a decrease in excitation and a possible increase in inhibition taking place within a narrow temporal window. Thus, our results support the hypothesis that anti-hebbian plasticity at the parallel fibre synapse mediates the generation of negative images of predicted sensory input in these structures. □

Methods

400-μm thick slices of the mormyrid electrosensory lobe were maintained in an interface chamber in humidified 95% O_2, 5% CO_2 and superfused at room temperature (23–25 °C) with artificial cerebropsinal fluid (ACSF), at a rate of 2 ml min^{-1}. The ACSF was saturated with 95% O_2, 5% CO_2 and contained (in mM): NaCl 124; KCl 2.0; KH_2PO_4 1.25; $CaCl_2$ 2.6; $MgSO_4.7H_2O$ 1.6; $NaHCO_3$ 24; glucose 20. Two monopolar insulated tungsten stimulation electrodes were placed in the molecular layer (S1 and S2; inset in Fig. 1a) in order to stimulate two separate parallel fibre inputs to the recorded neurons (pulses of 0.1 ms and 5–50 μA amplitude). Purkinje-like cells were recorded intracellularly with sharp microelectrodes (150–200 MΩ) containing 2% biocytin dissolved in 2M potassium methyl sulphate. Paired pulse facilitation was measured in 7 cells at interpulse delays of 30–45 ms in order to test for activation of separate groups of fibres by S1 and S2. Facilitation was marked with stimulus pairs S1–S1 (range, 27–108%; mean, 54%) or S2–S2 (range, 18–69%; mean, 42%) but was minimal or absent with stimulus pairs S1–S2 (range, −7 to 13%; mean, −1.3%) or S2–S1 (range, −15 to 3%, mean, −3.6%), indicating that separate groups of fibres were stimulated.

Received 9 September 1996; accepted 24 March 1997.

1. Bell, C. An efference copy which is modified by reafferent input. *Science* **214,** 450–453 (1981).
2. Montgomery, J. & Bodznick, D. An adaptive filter than cancels self-induced noise in the electrosensory and lateral line mechanosensory systems of fish. *Neurosci. Lett.* **174,** 145–148 (1994).
3. Bastian, J. Pyramidal cell plasticity in weakly electric fish: A mechanism for attenuating responses to reafferent electrosensory inputs. *J. Comp. Physiol.* **176,** 63–78 (1995).
4. Montgomery, J., Coombs, S., Conley, R. & Bodznick, D. Hindbrain sensory processing in lateral line, electrosensory, and auditory systems: a comparative overview of anatomical and functional similarities. *Aud. Neurosci.* **1,** 207–231 (1995).
5. Bell, C., Caputi, A., Grant, K. & Serrier, J. Storage of a sensory pattern by anti-Hebbian synaptic plasticity in an electric fish. *Proc. Natl Acad. Sci. USA* **9,** 4560–4654 (1993).
6. Bell, C., Bodznick, D., Montgomery, J. & Bastian, J. The generation and subtraction of sensory expectations within cerebellum-like structures. *Brain, Behav. Evol.* (in the press).
7. Nelson, M. & Paulin, M. Neural simulations of adaptive reafference suppression in the elasmobranch electrosensory system. *J. Comp. Physiol. A* **177,** 723–736 (1995).
8. Meek, J. *et al.* Interneurons of the ganglionic layer of the mormyrid electrosensory lateral line lobe: morphology, immunocytochemistry and synaptology. *J. Comp. Neurol.* **375,** 43–65 (1996).
9. Grant, K. *et al.* Projection neurons of the mormyrid electrosensory lateral line lobe. *J. Comp. Neurol.* **375,** 18–42 (1996).
10. Sakurai, M. Synaptic modification of parallel fiber-Purkinje cell transmission in *in vitro* guinea-pig cerebellar slices. *J. Physiol.* **394,** 463–480 (1987).
11. Hirano, T. Differential pre- and postsynaptic mechanisms for synaptic potentiation and depression between a granule cell and a Purkinje cell in rat cerebellar cultures. *Synapse* **7,** 321–323 (1991).
12. Gustafsson, B., Wigström, H., Abraham, W. & Huang, Y. Long term potentiation in the hippocampus using depolarizing current pulses as the conditioning stimulus to single volley synaptic potentials. *J. Neurosci.* **7,** 774–780 (1987).
13. Debanne, D., Gähwiler, B. & Thompson, S. Asynchronous pre- and postsynaptic activity induces associative long-term depression in area CA1 of the rat hippocampus *in vitro*. *Proc. Natl Acad. Sci. USA* **91,** 1148–1152 (1994).
14. Stanton, P. & Sejnowski, T. Associative long term depression in the hippocampus induced by Hebbian covariance. *Nature* **339,** 215–218 (1989).
15. Hashemzadeh-Gargari, H., Colbert, C. & Levy, W. Refining the temporal defining of an association at the neuronal level using long-term potentiation and long-term depression in the dentate gyrus. *Neurosci. Lett.* **126,** 37–40 (1991).
16. Huerta, P. & Lisman, J. Bidirectional synaptic plasticity induced by a single burst during cholinergic theta oscillation in CA1 *in vitro*. *Neuron* **15,** 1053–1063 (1995).
17. Ito, M. Long term depression. *Annu. Rev. Neurosci.* 85–102 (1989).
18. Chen, C. & Thompson, R. Temporal specificity of long-term depression in parallel fiber-Purkinje synapses in rat cerebellar slice. *Learning Mem.* **2,** 185–198 (1995).
19. Ekerot, C. & Kano, M. Stimulation parameters influencing climbing fibre induced long-term depression of parallel fibre synpases. *Neurosci. Res.* **6,** 264–268 (1989).
20. Markram, H., Lübke, J., Frotscher, M. & Sakmann, B. Regulation of synaptic efficacy by coincidence of postsynaptic APs and EPSPs. *Science* **275,** 213–215 (1997).
21. Hebb, D. The organization of behavior. (Wiley, New York, 1949).

Acknowledgements. We thank Y. Fregnac for discussion and Y.F, N. Barmack and R. Kramis for critical reviews of the manuscript. This research was supported by grants from the NSF and the National Institute of Mental Health (to C.B.), by a contract from the European Economic Community, a grant from NATO and funds from the Centre National de Recherche Scientifique (to K.G.), and by grants from the del Duca Foundation and Yamada Science Foundation (to Y.S.).

Correspondence and requests for materials should be addressed to C.C.B. (e-mail: bellc@lhs.org).

Dynamics of orientation tuning in macaque primary visual cortex

Dario L. Ringach, Michael J. Hawken & Robert Shapley

Center for Neural Science, New York University, 4 Washington Place, New York, New York 10003, USA

Orientation tuning of neurons is one of the chief emergent characteristics of the primary visual cortex, V1 (refs 1, 2). Neurons of the lateral geniculate nucleus, which comprise the thalamic input to V1, are not orientation-tuned, but the majority of V1 neurons are quite selective. How orientation tuning arises within V1 is still controversial[1,3–17]. To study this problem, we measured how the orientation tuning of neurons evolves with time[18–20] using a new method: reverse correlation in the orientation domain. Orientation tuning develops after a delay of 30–45 milliseconds and persists for 40–85 ms. Neurons in layers 4Cα or 4Cβ, which receive direct input from the thalamus, show a single orientation preference which remains unchanged throughout the response period. In contrast, the preferred orientations of output layer neurons (in layers 2, 3, 4B, 5 or 6) usually change with time, and in many cases the orientation tuning may have more than one peak. This difference in dynamics is accompanied by a change in the sharpness of orientation tuning; cells in the input layers are more broadly tuned than cells in the output layers. Many of these observed properties of output layer neurons cannot be explained by simple feedforward models[1,3–6], whereas they arise naturally in feedback networks[7–17]. Our results indicate that V1 is more than a bank of static oriented filters; the dynamics of output layer cells appear to be shaped by intracortical feedback.

We adapted the reverse correlation method[21] to study the dynamics of orientation tuning in macaque V1. The stimulus was generated as follows. For each cell, a set $\mathcal{S}$ of sinusoidal gratings of a fixed spatial frequency but different orientations and spatial phases was generated. In these experiments, the orientation domain was sampled in steps ranging between 3° and 12°. For each orientation, sinusoidal gratings at four spatial phases a quarter of a cycle apart were included in the set. A stochastic image sequence (the stimulus) was generated by randomly selecting, at each video refresh time, a new image from $\mathcal{S}$. This was done at a rate of 60 frames per second for a period of 15 min.

The data were analysed to determine the dependence of the cell's response on the past history of oriented gratings presented on its receptive field (Fig. 1). First, an array of counters corresponding to each of the orientations present in the stimulus was zeroed. A fixed value of a time-delay parameter τ was selected. For each nerve impulse recorded, we went back τ ms in time and obtained the orientation of the grating that was present at that moment in the image sequence. The counter corresponding to that orientation was incremented by one. Gratings at the same orientation but different spatial phases shared the same counter. Thus, this procedure averaged across spatial phases. When all action potentials were distributed in the counters, we normalized the resulting histogram by their total number and thereby obtained an estimate of the probability that an orientation θ was present in the stimulus image sequence τ ms before a nerve impulse was generated by the cell. This probability is denoted by $r_\tau(\theta)$. For a fixed value of τ, the function $r_\tau(\theta)$ is a probability distribution on the orientation angles present in the stimulus set. Note that this procedure is equivalent to that of computing the forward correlation: the probability of firing of a cell τ ms after the presentation of a particular orientation in the